Annals of Glaciology 15 1991

The propagation of characteristics in sea-ice deformation fields

BJÖRN ERLINGSSON
Norwegian Polar Research Institute, P.O. Box 158, N-1330 Oslo Lufthavn, Norway
and Institute of Geophysics, University of Oslo, P.O. Box 1022, N-0315 Blindern, Oslo 3, Norway

ABSTRACT. The role of internal forces in determining the geometrical properties of local features such as leads and ridges in sea ice has been investigated. A description of the horizontal stress distribution in a granular material subject to two-dimensional deformations has been derived. The description yields expressions for the propagation of deformation characteristics in a granular deformation field with constant angle of internal friction. The characteristics are mathematical singularities interpreted as trajectories of constant state variables, e.g. ice concentration or ice thickness typified as leads, fractures, pressure and shear ridges. The derived descriptions are used to study the geometrical nature of curving and rectilinear lead patterns frequently observed in sea-ice deformation fields. An expression for the relationship between the arching (tangent angling) of characteristics and relative increase in shear (maximum shear stress) along them is derived. It is explained how the acute angle between large-scale rectilinear characteristics is related to the important mechanical property of the deformed material, the angle of internal friction. It is outlined how the derived results can be applied to study the horizontal distribution of internal forces in sea ice by using imagery data and stress measurements at one site only.

INTRODUCTION

Uniform patterns of fractures, leads, faults and pressure ridges are an important and prominent property of materials being subjected to deformations in the Earth's crust, outlet glaciers and sea ice. These patterns characterize a material's mechanical properties and the physical conditions with respect to internal forces in the deformation field. The internal forces in sea ice arise as a response to external loads; e.g. surface tractions due to relative wind and sea-current friction, sea-surface tilt and accelerations. The ice resistance to deformations is determined by the interaction between the ice floes or rigidly moving clusters of ice floes, here denoted simply as the rigid elements of the deformation field. The horizontal deformations cause the ice to ridge and raft, or they may open or close the leads. The internal forces are important for the drift of the ice cover. Horizontal deformations and the associated ice ridging and rafting play the fundamental role in determining the distribution of ice thickness, which in itself controls heat fluxes between the ocean and atmosphere and ice production. This is an important agent in the formation of the global climate. Furthermore, during the passage of anomalous atmospheric-pressure fields, the internal forces in the sea-ice field present one of the most hazardous conditions for constructions in the sea-ice field.

Quite contrary to the division into molecular and macroscopic scales in other geophysical fluids, the division into large and small scales in sea ice is far from clear. The expressions derived for the general description of the deformation phenomena must account for this, otherwise there is hardly any hope for describing and explaining important features and their geometrical properties. The common nature of the features which are associated with irreversible deformations is that they represent discontinuities, or infinite horizontal strains or strain rates, with respect to an infinite small measure of length or time. The spatial derivatives of the velocity field are, therefore, discontinuous or infinite, coinciding with the so-called characteristics of the strain field. The objective of the present study is to obtain an understanding and a description of the propagation of deformation characteristics in sea ice and to see how these can be used to explain and interpret observed natural phenomena.

Marco and Thomson (1977) and Sodhi (1977) reported rectilinear diamond-shaped lead patterns observed in the Beaufort and Chukchi seas, respectively. Vinje and Finnekåsa (1986) measured the length and width of large (5–200 km) parallelepiped-shaped "ice floes" or coherent clusters of ice floes drifting rigidly through the Fram Strait. The measurements of the length and width of the clusters revealed a distinct linearly-correlated relationship (correlation coefficient

https://doi.org/10.3189/1991AoG15-1-73-80 Published online by Cambridge University Press

0.89). The high correlation between the length and width for lengths ranging from 5–200 km suggests a fixed value of the acute or steepest angle of the ice floes corresponding to $\beta = 32° \pm 2°$. Barry and others (1989) reported large-scale (500 km) uniform and continuous curving lead patterns (in SMMR images) in the central Arctic, similar to those also evident on a smaller scale (5 km, in IR images) reported by Ketum and Wittmann (1972) in newly frozen ice off the Greenland coast. These patterns occur for a wide range of scales, prompting us to seek an explanation on the basis of a sound physical formulation of the deformation phenomena in sea ice.

A material fails (fractures or flows) in response to external loads, causing internal stresses that exceed their yield strength. A macroscopic description of the interaction between the rigid elements in the deformation fields yields an expression for the acute intersection angles between deformation features, such as leads, and pressure and shear ridges, generated by the same external loads, or better understood as the primary stress field. The possible intersection angles are functions of the angle of internal friction, to which an unknown breaking index is assigned (Erlingsson, 1988). The breaking index associated with the above rectilinear features, rendering an angle of internal friction consistent with analysis of the deformation patterns, was $i = 2$ (Erlingsson, 1988). This interpretation of the rectilinear features is at variance with the interpretation given by Marco and Thomson (1977) and Sodhi (1977). The discrepancy concerns the ambiguities associated with the breaking indices, where the breaking index (implicitly) "assigned" to the features by Marco and Thomson (1977) and Sodhi (1977) was $i = 1$, giving twice as high a value for the angle of internal friction. The question addressed here is, therefore: can the geometrical properties in terms of the curvature of the deformation or velocity or deformation characteristics be interpreted in terms of a sound physical model? Furthermore, what causes the peculiar geometric features and how are they related to the physical conditions, the external loads and the properties of the material in the deformation field?

The present knowledge of fragmentation processes, which are scale invariant and stochastic in nature, implies that the complete determination of the general displacement pattern in a deformed material is still out of reach. The prerequisites for deformations are: the internal stresses must fulfil the criteria of failure (fracture and flow), and the external loads and body forces are sufficiently high to cause the material to yield. Deformation processes are irreversible in nature, and it is assumed here that the deformation of a material can be stopped or started at any instant simply by turning off or on the external loads. This means that the mechanical properties of the material are invariant under the deformation process. The elastic (reversible distortion) properties of the material are neglected and the dimensions of the disturbances and displacements are considered to be infinitely small with respect to the characteristic dimension of the deformation field being studied.

Below, we will use the method of characteristics to derive descriptions of the propagation of curvilinear or rectilinear features in two-dimensional deformation fields. Characteristics are mathematical inventions which allow for certain differential quotients to be discontinuous across curves along which the equations can be integrated as ordinary differential equations. This makes it easy for us to associate the characteristics with prominent features in sea-ice deformation fields; e.g. leads, and pressure and shear ridges. The method of characteristics is essentially finding these curves, which are associated with a particular system of partial differential equations along which a certain property (constant or an integral) is preserved. This property is inherent to the system of equations applied to the description of the phenomenon of study. In our case, the system of equations consists of the momentum balance in two dimensions and a stress criterion for failure (fracture or flow) in the material. We will see from the physical formulation of the problem how the mathematical characteristics can be interpreted in terms of observable features and which properties are preserved along them.

BASIC CONCEPTS

The stress on an element surface is decomposed into projections along its normal, the normal stress σ_n, and the remaining part along the surface, the shear stress τ_n. The normal stresses σ_n and the shear stresses τ_n, on elements with surface normal $\mathbf{n}$ can be expressed by the equation for the Mohr's circle with centre at $(-\Pi, 0)$ and radius Γ : $(\Pi - \sigma_n)^2 + \tau_n^2 = \Gamma^2$ in which Π and Γ are the stress invariants

$$\Pi = \frac{\sigma_{xx} + \sigma_{yy}}{2}, \qquad (1)$$
$$\Gamma^2 = \left(\frac{\sigma_{xx} - \sigma_{yy}}{2}\right) + \sigma_{xy}^2$$

and σ_{xx}, σ_{yy} and σ_{xy} are the normal and shear stresses with respect to the Cartesian x and y axes, respectively. In two dimensions, these invariants are the *isotropic pressure*, Π, and the *shear*, Γ. Note that Π and Γ are often referred to as σ_I and σ_{II}, respectively. We chose the former here to avoid confusion with the the σ_1 and σ_2, the principal (maximum and minimum) stresses.

In order for the material to (fail) flow or fracture a yield criterion is postulated. In the so-called shear-stress criterion, the modulus of the shear stress, $|\tau_n|$, is expressed as a functional relationship of the form

$$|\tau_n| = f(\sigma_n, A_i) \qquad (2)$$

where A_i are any other variables, e.g. concentration, ice thickness, cohesion, that might influence the state of yield. They will be referred to here as state variables. Such criteria specify the orientation of the yield surface or the slip lines (Erlingsson, 1988). Because of the Mohr circle property, one may write

$$\tau_n = \Gamma \sin 2\theta, \qquad \sigma_n = -\Pi + \Gamma \cos 2\theta\,. \qquad (3)$$

Equation (2) can be rewritten formally as

$$\Gamma = \widehat{\Gamma}(\Pi, A_i) \qquad (4)$$

(henceforth the hat will be omitted). This form of the yield criterion is particularly convenient for the maxi-

https://doi.org/10.3189/1991AoG15-1-73-80 Published online by Cambridge University Press

mum shear-stress criterion. The most important mechanical property of the deformable materials employed here is the angle of internal friction, which is defined by the slope of the Mohr's envelope $f(\sigma_n, A_i)$,

$$\frac{\mathrm{d}f(\sigma_n, A_i)}{\mathrm{d}\sigma_n}|_{A_i} \equiv -\tan\phi = \cot 2\lambda\,, \tag{5}$$

where the so-called deflection angle is $\lambda = (\pi/4) + (\phi/2)$. It can be shown to be related to the slope of the maximum shear stress curve by

$$\frac{\partial\Gamma(\Pi, A_i)}{\partial\Pi} = \sin\theta = -\cos 2\lambda\,. \tag{6}$$

The principal direction of stress or strain of a particular rigid element is not a directly observable quantity. However, a failure-stress state at a certain place leads to a set of possible propagation directions, θ_j, or principal directions of rigid elements. The principal directions of the different rigid elements are, therefore, observable indirectly as the orientations of a particular observable deformation feature (e.g. fractures, leads, slip lines or faults and pressure ridges) associated with the deformation field. Possible propagation directions of mechanically similar features are interrelated by the so-called primary (principal) direction, θ_0, the branching index, j, and the deflection angle, λ, where (Erlingsson, 1988)

$$\theta_j = \theta_0 + 2j\lambda, \qquad j = 0, \pm 1, \pm 2, \ldots \tag{7}$$

The reference orientation for the feature is related to the associated primary principal direction and its mechanical nature. A pressure ridge, for example, is orientated parallel to the direction of maximum normal stress. In the same manner, a shear ridge represents a slip line elongated in the direction that makes the angle $-\lambda$ (or λ) with the principal direction of the associated rigid element (Erlingsson, 1988). In other words, the propagation of any feature can be related to the distribution of primary principal direction, if the associated branching index is known. The distribution of the primary principal direction in the (x, y)-plane can be used to describe the orientation of any feature in the (x, y)-plane with a particular branching index.

It is known from classical continuum mechanics that the components of the two-dimensional symmetric stress tensor, $\boldsymbol{\sigma}$, can be expressed in terms of the positive valued invariants Π and Γ, and the principal direction, Θ, which is the angle between the x axis and the direction of the maximum normal stress of a particular element.

$$\begin{aligned} \sigma_{xx} &= -\Pi + \Gamma\cos 2\Theta\,, \\ \sigma_{yy} &= -\Pi - \Gamma\cos 2\Theta\,, \\ \sigma_{xy} &= \Gamma\sin 2\Theta\,. \end{aligned} \tag{8}$$

This must hold for every element in the deformation field, and this presentation is invariant under the transformation $\Theta \to \Theta + n\pi$, so that

$$\boldsymbol{\sigma}(\Pi, \Gamma, \Theta) = \boldsymbol{\sigma}(\Pi, \Gamma, \Theta + n\pi), \qquad n = 0, \pm 1, \pm 2, \ldots \tag{9}$$

The equations of motion in the (x, y)-plane can be expressed as a balance between the internal forces, described as the divergence $\nabla\cdot\boldsymbol{\sigma}$, and the external loads as the sum of the in plane surface tractions and accelerations, $\mathbf{a}$, viz.,

$$\nabla\cdot\boldsymbol{\sigma} + \mathbf{a} = 0 \tag{10}$$

Equation (10) can be simplified markedly by transforming it into curvilinear coordinates $s_1(x, y)$ and $s_2(x, y)$, of which tangents coincide with the primary and the first induced slip lines making the angle $-\lambda$ and $+\lambda$ with respect to the principal direction (see Erlingsson, 1988 and Fig. 1). The associated coordinate unit tangent vectors, $\mathbf{e}_1$ and $\mathbf{e}_2$, are expressible in terms of the Cartesian base vectors according to

$$\mathbf{e}_j = \cos\theta_j\mathbf{i}_x + \sin\theta_j\mathbf{i}_y, \quad \text{where } \theta_{1,2} = \Theta \mp \lambda. \tag{11}$$

The corresponding Jacobian, $J = \cos\phi$, does not vanish as long as the material can be expected to be of finite shear strength, i.e. if $|\tau_n| < \infty$ for all σ_n, therefore $\phi < \pi/2$ and $J \neq 0$. The external and internal forces can be projected on the new coordinate vectors $\mathbf{e}_1$ and $\mathbf{e}_2$. A linear combination of these projections ($\cos\phi \neq 0$) yields a simplified version of the equations of motion, expressed in terms of the three dependent variables Π, Γ, and Θ. Referred to the curvilinear slip-line coordinates s_1 and s_2 they read:

$$\begin{aligned} \frac{\partial\Pi}{\partial s_1} - \sin\phi\frac{\partial\Gamma}{\partial s_1} + 2\Gamma\cos\phi\frac{\partial\Theta}{\partial s_2} &= \mathrm{a}_1\cos^2\phi\,, \\ \frac{\partial\Pi}{\partial s_2} - \sin\phi\frac{\partial\Gamma}{\partial s_2} - 2\Gamma\cos\phi\frac{\partial\Theta}{\partial s_2} &= \mathrm{a}_2\cos^2\phi\,, \end{aligned} \tag{12}$$

where a_1 and a_2 are the components of the external loads and accelerations in the new coordinate system. The slip lines $s_1(x, y)$ and $s_2(x, y)$ are themselves geometrically related to the failure of the deforming material, and can be found by solving the Cauchy initial value problem, and their slopes are given by

$$\frac{\mathrm{d}s_{1,2}}{\mathrm{d}y} = \tan(\Theta \mp \lambda)\,. \tag{13}$$

The momentum equations (12) comprise the three unknown variables Π, Γ and Θ. They are complemented by the yield stress criterion and the equations of state, relating the state variables to the unknowns, if such relations are needed.

The yield criterion for sea ice is currently poorly known. Nevertheless, sea ice evidently behaves as a granular material with constant angle of internal friction for a wide range of scales (Erlingsson, 1988). Among the state variables, presumably the most important ones are ice thickness, ice concentration and horizontal cohesion. They are known to be varying very much in a typical ice field. Clearly, Equation (6) implies that

$$\frac{\partial\Gamma}{\partial s} = \sin\phi\frac{\partial\Pi}{\partial s} + \frac{\partial A_j}{\partial s}\frac{\partial\Gamma}{\partial A_j}\,, \tag{14}$$

which, when introduced into the momentum equation, reduces the number of extrinsic dependent variables by

https://doi.org/10.3189/1991AoG15-1-73-80 Published online by Cambridge University Press

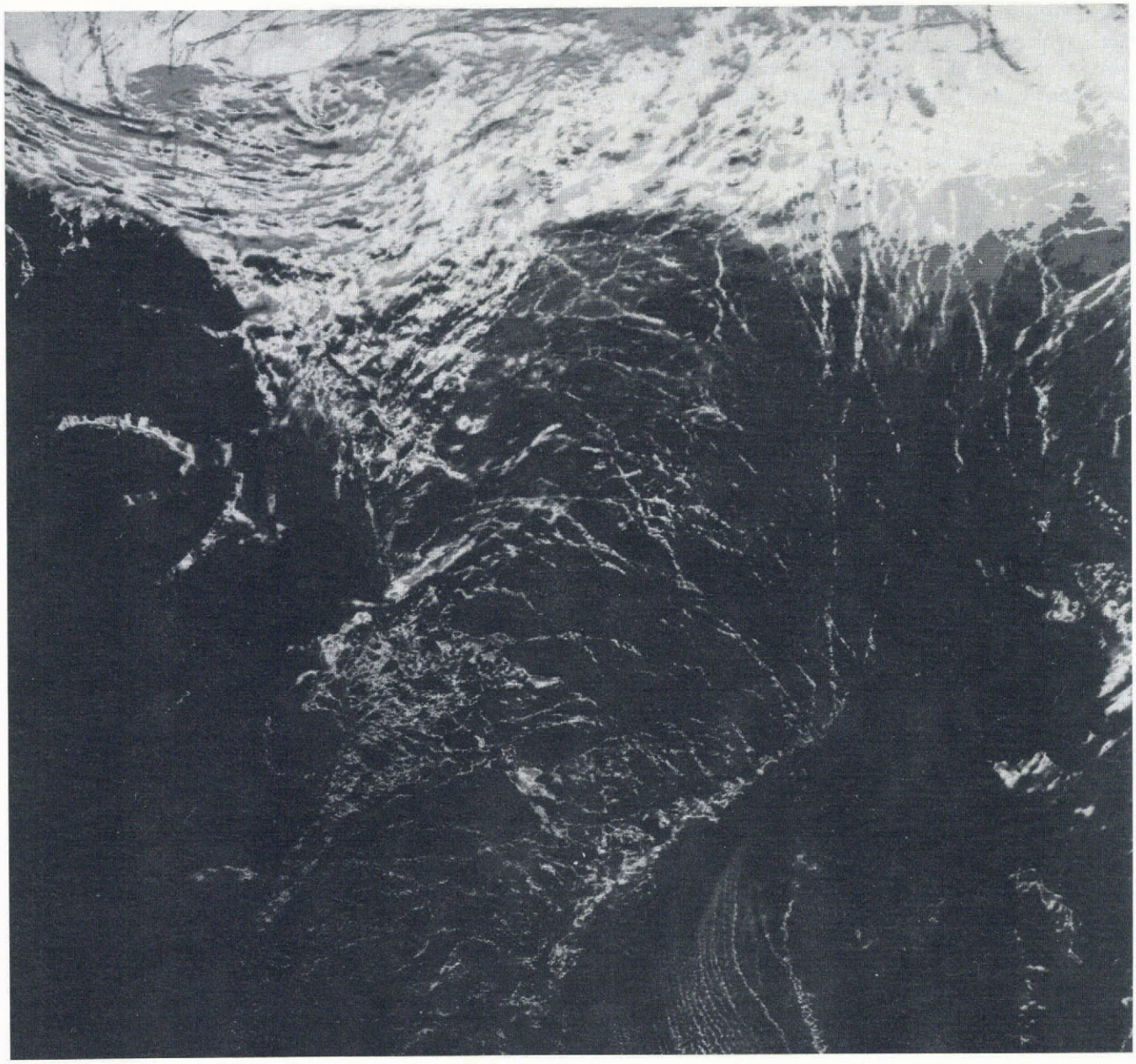

Fig. 1. An AVHRR visible image from the Fram Strait between Greenland and Svalbard showing curvilinear and rectilinear lead patterns (characteristics) in the sea-ice field (see cover of this issue for colour version). The width of Fram Strait is approximately 300 km.

one and brings about the intrinsic variables: the angle of internal friction ϕ, and the unspecified state variables A_j, by the last term on the righthand side of Equation (14).

The treatment of the state variables complicates the problem. They are generally not well known; nor is it their exact implication for the mechanical state of the material. To eliminate their contribution here for the sake of simplicity one must either introduce an equation for the relation between the state variables associated with $\partial\Gamma/\partial A_j$, or one must constrain their spatial distribution by setting $\partial A_i/\partial s_j$ $(j = 1, 2)$ to zero implying A_i = constant along any slip-line curve. This removes all the state variables from the problem, leaving only the angle of internal friction as a variable. An analogous result is achieved by assuming a cohesion-free material of constant angle of internal friction, the so-called ideal granular material. Indeed, Equation (6), subject to ϕ = constant, implies $\Gamma(\Pi = 0, A_i)$ = constant and therefore $\partial\Gamma/\partial A_i = 0$, which eliminates the last term on the righthand side of Equation (14). These conditions can be understood when interpreting the slip-line curves, which, as shown below, are mathematical characteristics. Trajectories of accrued features such as leads, and pressure and shear ridges do evolve along curves of constant state variables such as ice thickness or concentration. Similarly, in a granular material with vanishing cohesion, distinct features follow the typical pattern of the characteristic lines. Examples are open leads, fractures, and active pressure and shear ridges, where disintegration of the rigid elements occurs with the associated disappearance of cohesion.

https://doi.org/10.3189/1991AoG15-1-73-80 Published online by Cambridge University Press

Using Equation (14) for a granular material with vanishing cohesion, Equations (12) subject to $\cos\phi \neq 0$ become

$$\cot\phi\frac{\partial\Gamma}{\partial s_1} + 2\Gamma\frac{\partial\Theta}{\partial s_1} = \mathrm{a}_1\cos\phi\,,$$
$$\cot\phi\frac{\partial\Gamma}{\partial s_2} - 2\Gamma\frac{\partial\Theta}{\partial s_2} = \mathrm{a}_2\cos\phi. \qquad (15)$$

These equations are to be complemented by Equation (13). We solve them below and use the solution to interpret the propagation of features in the (x, y)-plane. Equations (15) can be written in terms of dimensionless quantities s', a' and Γ', normalized by typical values for length, external forces, and shear l^*, a^* and Γ^*, respectively, where

$$s_j{}'l^* = s_j\,,$$
$$\mathrm{a}_j{}'\mathrm{a}^* = \mathrm{a}_j\,, \qquad j = 1,2; \qquad (16)$$
$$\Gamma'\Gamma^* = \Gamma\,.$$

Writing Equations (15) in terms of these shows that geometrical and dynamical similarity is achieved provided that

$$\mathrm{a}^* l^* (\Gamma^*)^{-1} = 1\,. \qquad (17)$$

Interestingly, for a typical maximum shear stress associated with a particular deformation phenomenon (e.g. ridging of sea ice of particular thickness or type), Γ^*, the long-range transfer of loads (l^*: large) is associated with small external loads (a^*: small) and vice versa. The estimated characteristic length scales associated with ridging of 0.5–3.5 m-thick ice and external loads corresponding to wind speeds of $3 - 15\,\mathrm{m\,s^{-1}}$ are $l^* = 0.4 - 400\,\mathrm{km}$ (Erlingsson, 1989). This means that during the passage of anomalous atmospheric pressure fields, the suitable means for observing deformation phenomena are photography from sustained platforms as well as satellite imagery.

STRESS ALONG CHARACTERISTICS

The propagation of the families of curves $s_j(x, y) =$ constant $(j = 1, 2)$ is described by the solution of the Cauchy initial value problem of Equations (15). They are hyperbolic and the Method of Characteristics (further denoted as MoC, see Abbott, 1962) is applied to solve them. The MoC allows them to be written as *ordinary differential equations* for the dependent variables along the characteristics which are families of the coordinate curves, $\{s_1(x,y) : s_2(x,y) = \text{const.}\}$ and $\{s_2(x,y) : s_1(x,y) = \text{const.}\}$:

$$\mathrm{d}\Gamma + 2\tan\phi\,\Gamma\mathrm{d}\Theta = \sin\phi\,\mathrm{a}_1\mathrm{d}s_1, \quad \text{where } s_2 = \text{const.},$$
$$\mathrm{d}\Gamma - 2\tan\phi\,\Gamma\mathrm{d}\Theta = \sin\phi\,\mathrm{a}_2\mathrm{d}s_2, \quad \text{where } s_1 = \text{const.}, \qquad (18)$$

or after rearrangement

$$\frac{\mathrm{d}}{\mathrm{d}s_1}(\Gamma\mathrm{E}) = \mathrm{E}\sin\phi\,\mathrm{a}_1\,, \quad \text{where } s_2 = \text{const.}\,,$$
$$\frac{\mathrm{d}}{\mathrm{d}s_2}(\Gamma\mathrm{E}^{-1}) = \mathrm{E}^{-1}\sin\phi\,\mathrm{a}_2\,, \quad \text{where } s_1 = \text{const.}\,, \qquad (19)$$

where

$$\mathrm{E}(\Theta) = \exp(2\tan\phi\,\Theta)\,, \qquad (20)$$

the so-called *arching function*, has been introduced. From this, straightforward integration yields

$$\Gamma\mathrm{E} = \mathrm{I}_1(s_1),\ \mathrm{I}_1(s_1) = \sin\phi\int_{s_{10}}^{s_1}\mathrm{E}\mathrm{a}_1\mathrm{d}s_1 + \Gamma_1\mathrm{E}(\Theta_1)\,,$$
$$\Gamma\mathrm{E}^{-1} = \mathrm{I}_2(s_2),\ \mathrm{I}_2(s_2) = \sin\phi\int_{s_{20}}^{s_2}\mathrm{E}^{-1}\mathrm{a}_2\mathrm{d}s_2 + \Gamma_2\frac{1}{\mathrm{E}(\Theta_2)}\,, \qquad (21)$$

in which Θ_1, Θ_2 and Γ_1, Γ_2 are values Θ and Γ at the initial points at s_{10} and s_{20} on the s_1 and s_2 characteristics, respectively. The characteristic slopes can most easily be deduced from Equations (19) which imply

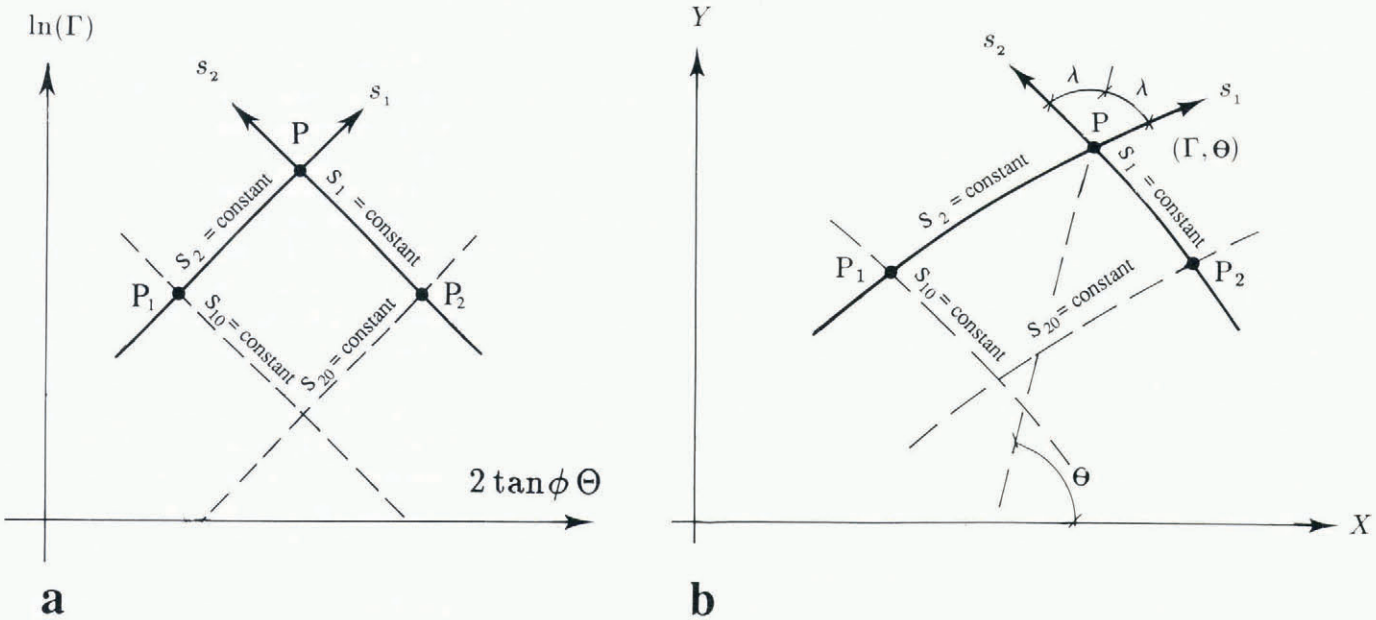

Fig. 2. The characteristics on (a) the $2\tan\phi\,\Theta - \ln\Gamma$ diagram and (b) the corresponding (x,y)-plane.

https://doi.org/10.3189/1991AoG15-1-73-80 Published online by Cambridge University Press

$$\frac{\mathrm{d}\ln\Gamma}{\mathrm{d}\ln \mathrm{E}} = \frac{\mathrm{d}\ln\Gamma}{\mathrm{d}(2\tan\phi\ \Theta)} = \pm 1\,. \tag{22}$$

In the $(2\tan\phi\ \Theta, \ln\Gamma)$-plane they represent straight lines inclined at $\pm 45°$ (Fig. 2). The shear, Γ, and the principal direction, in terms of the arching E (Θ) at a particular point, P, at which the (s_1, s_2)-curves intersect, are given by

$$\Gamma^2 = \mathrm{I}_1(s_1)\mathrm{I}_2(s_2), \quad \mathrm{E}(2\Theta) = \frac{\mathrm{I}_1(s_1)}{\mathrm{I}_2(s_2)}. \tag{23}$$

The point P_1 and the corresponding shear and principal direction (Γ_1, Θ_1) is where the characteristics $\{s_1 : s_2 = \text{const.}\}$ and $\{s_{20} : s_{10} = \text{const.}\}$ intersect and P_2 is where the characteristics $\{s_{10} : s_{20} = \text{const.}\}$ and $\{s_2 : s_1 = \text{const.}\}$ intersect (Fig. 2). The principal directions and shears at P_1 and P_2 are solutions of Equations (21) where, from Equations (23) one finds

$$\begin{aligned} {\Gamma_1}^2 &= \mathrm{I}_1(s_1)\mathrm{I}_2(s_{20}), \quad \mathrm{E}(2\Theta_1) = \frac{\mathrm{I}_1(s_1)}{\mathrm{I}_2(s_{20})}, \\ {\Gamma_2}^2 &= \mathrm{I}_1(s_{10})\mathrm{I}_2(s_2), \quad \mathrm{E}(2\Theta_2) = \frac{\mathrm{I}_1(s_{10})}{\mathrm{I}_2(s_2)}. \end{aligned} \tag{24}$$

Clearly, by multiplying and dividing Equations (23) by $\sqrt{\mathrm{I}_1(s_{10})\mathrm{I}_2(s_{20})}$ and using Equations (24), the shear Γ and principal direction at P, in terms of the arching $\mathrm{E}(\Theta)$ at P, are related to the initial values at P_1 and P_2

$$\Gamma^2 = \Gamma_1\Gamma_2\mathrm{E}(\Theta_1 - \Theta_2), \quad \mathrm{E}(2\Theta) = \frac{\Gamma_1}{\Gamma_2}\mathrm{E}(\Theta_1 + \Theta_2). \tag{25}$$

The two equations can now be combined to derive the relations between the arching and shear along each characteristic $s_1(x, y)$ and $s_2(x, y)$ in terms of the initial values at P_1 and P_2, i.e.

$$\begin{aligned} \Gamma &= \Gamma_1\mathrm{E}(\Theta - \Theta_1), \quad && \text{along } s_1\text{-characteristic}, \\ \Gamma &= \Gamma_2\mathrm{E}(\Theta_2 - \Theta), && \text{along } s_2\text{-characteristic}. \end{aligned} \tag{26}$$

Both equations can be combined for the characteristics s_1 and s_2, if we substitute $\Gamma = \Gamma_{1,2} + \Delta\Gamma, \Theta = \Theta_{1,2} + \Delta\Theta$ to obtain from (26)

$$\frac{(\Gamma + \Delta\Gamma)}{\Gamma} = \mathrm{E}(\pm\Delta\Theta). \tag{27}$$

The different signs are associated with the fact that the index $(j = 1, 2)$ is not known a priori; neither is the direction of increasing s_j along the physical characteristics (recall Equations (9) and (11)). Equations (26) are the *crucial statements* needed in numerical integration to interpret the shears from observed characteristics. Thus, knowing the absolute shear Γ at one site on a characteristic, its tangent deviation $\Delta\Theta$ can be measured and, therefore, it renders the shear (according to this model) as: $\Gamma + \Delta\Gamma = \Gamma\mathrm{E}(\pm\Delta\Theta)$, along the characteristic if the angle of internal friction is known (recall Equation (20)). In order to obtain the complete distribution of stresses in the plane one must interpolate from known measurement sites by integration along the characteristics according to Equation (27). Below we will estimate the propagation of characteristics in the (x, y)-plane.

PROPAGATION OF CHARACTERISTICS

The distribution of shear stress Γ in the (x, y)-plane is given by Equations (21) in terms of the principal direction Θ, along the characteristics of which the unit tangent vectors are functions of the principal direction and angle of internal friction according to Equations (11). A fundamental theorem of differential geometry asserts that a planar curve is uniquely defined by its curvature. For a granular material, those of the characteristics can be expressed through Equation (11) as functions of the principal direction. The vector representations of the $s_1(x, y)$-characteristic $\mathbf{r}_1(s_1)$ and of the $s_2(x, y)$-characteristic $\mathbf{r}_2(s_2)$ are described by the so-called Serret-Frenet formulae (Kreyszig, 1979)

$$\frac{\mathrm{d}\mathbf{r}_j}{\mathrm{d}s_j} = \mathbf{e}_j, \quad \frac{\mathrm{d}\mathbf{e}_j}{\mathrm{d}s_j} = \kappa_j\mathbf{n}_j, \quad \frac{\mathrm{d}\mathbf{n}_j}{\mathrm{d}s_j} = -\kappa_j\mathbf{e}_j\,, \tag{28}$$

where $j = 1, 2$ and $\mathbf{e}_j$ and $\mathbf{n}_j$ are the characteristics' unit tangent and normal vectors, respectively, and the curvature is defined by $\kappa_j = \mathrm{d}\Theta/\mathrm{d}s_j$, and on using Equations (18) and (26)), they can be related to the shear Γ and the components of the external loads a_1 and a_2 which themselves depend on ϕ = constant. Using Equations (21) the curvatures become

$$\kappa_j = (-1)^j\frac{\mathrm{a}_j}{4\Gamma}\cos\phi. \tag{29}$$

Parameterizing the sum of the external loads by their strength, a, and denoting the angle of intersection of this force with the x axis by α, the curvatures become

$$\kappa_{1,2} = \frac{\mathrm{a}}{4\Gamma}\sin(\Theta - \alpha \pm \lambda)\,. \tag{30}$$

The first of Equations (28) and the definition $\kappa = \mathrm{d}\Theta/\mathrm{d}s$ permit the characteristics to be integrated to yield

$$\mathbf{r}_j(\Theta') = \int_{\Theta_0}^{\Theta'}\frac{\mathbf{e}_j}{\kappa_j}\mathrm{d}\Theta + \mathbf{r}_j(\Theta_0), \qquad (j = 1, 2)\,. \tag{31}$$

Here, κ_j may be regarded as known functions of the principal direction Θ along the characteristics (see Equations (30) and (26)). Thus, knowing the sum of the external loads in terms of their strength, a, and the direction, α, and the initial values $\Gamma_{1,2}$ and $\Theta_{1,2}$, the propagation of characteristics is exactly given by Equation (31). But, even for uniform external loads, the integral of Equation (31) is not solvable in terms of known standard functions. However, Equations (26) can be used to obtain from a prescribed characteristic line the distribution of the shear, Γ, along it. Indeed, the curvature is known and, for a given external force field, a and α are known, and with known internal friction angle ϕ, λ and Θ are determined. Thus, Equation (31) allows evaluation of a and α if it is also assumed that they are uniformly distributed in the plane and that the shear is known at a single site.

Taylor series expansion of $\mathbf{r}_j(s_j)$ about s_{0_j} renders the so-called Canonical presentation of the characteristics that may be derived from the Serret-Frenet Equation (28):

https://doi.org/10.3189/1991AoG15-1-73-80 Published online by Cambridge University Press

$$\mathbf{r}_j(s_j) = \mathbf{r}_j(s_{j0}) + \left\{ S'_j - \kappa_{j0}^2 S_j'^3 \frac{1}{3!} \right\} \mathbf{e}_j + \left\{ \kappa_{j0} S_j'^2 \frac{1}{2!} + \frac{\mathrm{d}\kappa_{j0}}{\mathrm{d}s_j} S_j'^3 \frac{1}{3!} \right\} \mathbf{n}_j + \mathbf{o}(S_j'^3),$$

$$\text{where} \quad S'_j = S_j - S_{j0}. \tag{32}$$

By introducing orthogonal coordinates (x'_j, y'_j) with origin at (s_{10}, s_{20}), and with base vectors equal to the unit tangents and normals, respectively, one obtains

$$x'_j = S'_j - \kappa_j^2 S_j'^3 \frac{1}{3!} + \mathbf{o}(S_j'^3),$$
$$y'_j = \kappa_{j0} S_j'^2 \frac{1}{2!} + \frac{\mathrm{d}\kappa_{j0}}{\mathrm{d}s_j} S_j'^3 \frac{1}{3!} + \mathbf{o}(S_j'^3). \tag{33}$$

For a constant sum of external loads, because of Equations (26) and (30), the curvatures κ_j vary along the characteristics s_j as

$$\frac{\mathrm{d}\kappa_{1,2}}{\mathrm{d}s_{1,2}}|_{a,\alpha} = \{\cot(\Theta - \alpha \pm \lambda) \mp 2\tan\phi\}\kappa_{1,2}^2. \tag{34}$$

Note, non-linear terms in Equations (33) comprise first and higher order terms of the curvature. Furthermore, when the characteristics are straight line segments and the external forces are constant, then they remain so indefinitely. On the other hand, if the external loads are changing their orientation along the characteristics, changes in the curvature must also be expected even if characteristics should have been straight for some distance. Under these conditions the change in curvature due to the variation in the direction of the external loads is

$$\frac{\mathrm{d}\kappa_j}{\mathrm{d}s_j}|_{\kappa=0} = \frac{\mathrm{a}}{4\Gamma}\cos(\Theta - \alpha \pm \lambda)\frac{\mathrm{d}\alpha}{\mathrm{d}s_j}. \tag{35}$$

Accordingly, if the characteristics propagate as straight lines, then the maximum shear stress Γ and the *direction* of the sum of external loads and accelerations are constant along such lines. There are two families of such straight lines, characterized by Θ' and Θ'', respectively. They are asymptodes whose orientations in the (x, y)-plane, θ_j, are given by Equations (30) and (11),

$$\begin{aligned} \theta_1 &= \Theta' - \lambda, \quad \text{when} \quad \Theta' - \alpha + \lambda = n_1\pi, \\ \theta_2 &= \Theta'' + \lambda, \quad \text{when} \quad \Theta'' - \alpha - \lambda = n_2\pi, \\ &\quad \text{with} \quad n_{1,2} = 0, \pm 1, \pm 2, \ldots \end{aligned} \tag{36}$$

Accordingly, the acute intersecting angle between these families becomes the function of the angle of internal friction with breaking index $i = 2$ (see Erlingsson, 1988, equation (13) for explanations), i.e.

$$\beta = \min_l\{|(\theta_2 - \theta_1) - l\pi|\} = \min_l\{|4\lambda - l\pi|\} = \beta_2,$$
$$\text{where } l = 0, \pm 1, \pm 2, \ldots . \tag{37}$$

The curvatures of the characteristics diverge to infinity when the maximum shear stress approaches zero ($\Gamma \to 0$): i.e. characteristics converge to a single point in the plane when the shear vanishes. It follows that the shear along characteristics will always have the same (positive) sign when computing the solutions of this model for the physical plane. In summary, for a given characteristic and force field we have seen that the shear, Γ, can be computed. Having determined it along a characteristic, Equation (14), viz.

$$\frac{\partial\Gamma}{\partial s_j} = \sin\phi\frac{\partial\Pi}{\partial s_j} \tag{38}$$

permits us, through integration, to determine the isotropic pressure, Π, provided that it and the shear, Γ, are known at an initial point along that characteristic.

DISCUSSION AND CONCLUSIONS

The topic of this study has been the determination of the distribution of horizontal stresses and the propagation of characteristics in granular deformation fields. Its principal results concern the relation between the horizontal arching of the characteristics and the associated relative changes in maximum shear stress along them. The linear asymptotic behaviour of the deformation characteristics yields a definite breaking index ($i = 2$) for the rectilinear parallelepiped-shaped features, frequently observed in various deformation fields such as, for example, in sea ice and glacier ice. This enables unambiguous interpretation of the angle of internal friction from the geometry of such patterns. Furthermore, an explanation of the physical nature of these prominent deformation phenomena is proposed. The angle of internal friction corresponding to the observed geometry of such features in sea ice (Vinje and Finnekåsa, 1984) is $\phi = 16° \pm 2°$.

It was also demonstrated how deformation features, such as leads, shear and pressure ridges, in a somewhat regular array can be used in order to obtain, on the basis of a known internal friction angle, the stresses arising along these features. This opens a new perspective for the investigation of the mechanical behaviour of sea ice or glacier ice in real situations by using remote sensing imagery. On the other hand, using Equations (26), (33), and (35), the equations can be used to solve a classical Cauchy-initial value problem, provided the stress is given along a non-characteristic curve. Such applications with glaciological relevance will be reserved for a follow-up paper.

ACKNOWLEDGEMENTS

This work was carried out while the author held a scholarship from the National Science Foundation, Norway. The author expresses his grateful thanks to Kolumban Hutter for his excellent review and generous help while preparing the final manuscript of the paper. Thanks to Ron Lindsey at the Polar Science Center, University of Washington for kindly preparing the AVHRR-image in Figure 1.

REFERENCES

Abbott, M.C. 1966. *An introduction to the method of characteristics*. New York, American Elsevier.

Barry, R.G., M.W. Miles, R.C. Cianflone, G. Scharfen and R.C. Schnell. 1989. Characteristics of Arctic sea ice from remote-sensing data and their relationship to atmospheric processes. *Ann. Glaciol.*, **12**, 9–15.

https://doi.org/10.3189/1991AoG15-1-73-80 Published online by Cambridge University Press

Erlingsson, B. 1988. Two-dimensional deformation patterns in sea ice. *J. Glaciol.*, **34**(118), 301-308.

Erlingsson, B. 1989. Sea ice deformations in the proximity of coasts. *In* Axelsson, K.B.E. and L. A. Fransson, *eds. POAC 89. The 10th International Conference on Port and Ocean Engineering under Arctic Conditions, June 12–16, Luleå, Sweden. Proceedings. Vol. 3.* Luleå, Tekniska Högskolan i Luleå, 1349–1356.

Ketchum, R.D., *Jr*, and W.I. Wittmann. 1972. Recent remote sensing studies of the East Greenland pack ice. *In* Karlsson, T., *ed. Sea ice. Proceedings of an international conference ... Reykjavík, Iceland, May 10–13, 1971.* Reykjavík, National Research Council, 213–226.

Kreyszig, E. 1979. *Advanced engineering mathematics. Fourth edition.* New York, etc., John Wiley and Sons.

Marko, J.R. and R.E. Thomson. 1977. Rectilinear leads and internal motions in the ice pack of the western Arctic Ocean. *J. Geophys. Res.*, **82**(6), 979–987.

Sodhi, D.S. 1977. Ice arching and the drift of pack ice through restricted channels. *CRREL Rep.* 77-18.

Vinje, T.S. and O. Finnekåsa. 1986. The ice transport through the Fram Strait. *Nor. Polarinst. Skr.* 186.

The accuracy of references in the text and in this list is the responsibility of the author, to whom queries should be addressed.

https://doi.org/10.3189/1991AoG15-1-73-80 Published online by Cambridge University Press